JOURNAL OF GEOPHYSICAL RESEARCH, VOL. 96, NO. D3, PAGES 5369–5378, MARCH 20, 1991

Determination of Saharan Dust Radiance and Chlorophyll From CZCS Imagery

K. L. CARDER,[1] W. W. GREGG,[1,2] D. K. COSTELLO,[1] K. HADDAD,[3] AND J. M. PROSPERO[4]

An atmospheric correction algorithm is derived for oceanic areas of low chlorophyll *a* plus phaeophytin *a* concentrations ($\langle C \rangle \leq 0.25$ mg/m^3). The algorithm simultaneously corrects for the radiance effects of two different aerosol types observed in coastal zone color scanner (CZCS) imagery. The algorithm, called the two-component method, is applied to data from a time series of CZCS orbits during which both Saharan dust and a bluish haze were present. The method is evaluated by comparing the ocean chlorophyll concentrations after atmospheric correction to those measured in situ and to those determined by single-component methods from CZCS imagery. Reasonable agreement is found between the chlorophyll values estimated by the two-component method and in situ values, and the derived chlorophyll values for a Sargasso Sea region varied by less than 6% during a major influx of Saharan dust to the region. Aerosol and chlorophyll fields appeared confounded in imagery derived using single-component methods when multiple aerosol types were present, but no confounding was observed for imagery generated by the two-component method. The time series of aerosol radiance values due to Saharan dust was consistent with the changes in dust concentration and particle size measurements from an adjacent aerosol collection site on the Florida coast.

1. INTRODUCTION

Scattering by aerosols represents an important optical component of the atmosphere, which must be removed from Coastal Zone Color Scanner (CZCS) imagery before water-leaving radiances, and hence chlorophyll, may be determined. Furthermore, because of the temporal and spatial variability of the aerosol concentrations and their optical characteristics the proportion of the total radiance observed by the sensor which is due to aerosol scattering cannot be estimated and removed a priori as can Rayleigh scattering.

Up to 90% of the total radiance received at the CZCS sensor for most cloud-free scenes is due to the intervening atmosphere [*Gordon et al.*, 1983*a*]. Aerosol scattering may be responsible for 10–40% of the radiance. Yet the success of the CZCS atmospheric correction algorithms in estimating and subsequently removing these atmospheric effects is evident from their ability to determine the water-leaving radiance within about 10% for much of the world ocean and chlorophyll concentrations to within 30–40% [*Gordon et al.*, 1983*a*].

This accuracy is subject to some qualifications, however. The atmospheric correction algorithms have been most accurate during the first year (1978–1979) of CZCS operation before sensor degradation became significant and are most successful where a single aerosol type exists. Multiple aerosol types present in the same scene can confound these single-component atmospheric correction algorithms. Such a situation occurs with Saharan dust events. Major outbreaks of Saharan dust aerosols can be present as far west as Miami, Florida, especially during June, July, and August [*Prospero and Carlson*, 1972; *Savoie and Prospero*, 1977; *Carder et al.*, 1986]. Saharan dust differs in its spectral reflectance characteristics from the marine (sea salt) aerosols, and bluish hazes that are often present. A bimodal size distribution for marine aerosols (hydrated sea salts) has been observed, with the concentration and modal diameter for the larger fraction increasing with wind speed [*Patterson et al.*, 1980]. While the submicron fraction may exhibit blue-rich scatter, the scatter for the dominant large-particle fraction is not expected to be spectral. Near land, where small-particle sources are important [*Patterson et al.*, 1980], modified maritime hazes may exhibit blue-dominant scattering. In addition, small particles may be important above the marine boundary layer. Scattering by Saharan dust, which can contain rather large particles (volume distribution mode for this study was between 4 and 8 μm diameter [*Carder et al.*, 1986]), is unlikely to exhibit spectral scattering unless spectral absorption is significant. These aerosols absorb more strongly in the blue wavelengths [*Patterson*, 1981], however, and are consequently reddish-brown in color [*Prospero and Carlson*, 1972].

In this paper we present an algorithm to distinguish two aerosol types in an image and then determine their relative concentrations by observing the radiance contribution from each type at the satellite. The algorithm builds on the clear water radiance theory [*Gordon and Clark*, 1981] in which the water-leaving radiance values for all CZCS channels except the blue (443 nm) can be designated a priori when chlorophyll concentrations are less than 0.25 mg/m^3. Such is often the case in the summer away from coastal areas. We demonstrate the effectiveness of the "two-component" method by observing a time series of CZCS images in late June 1980 when an outbreak of Saharan dust passed over Florida. During this period, chlorophyll pigment concentrations were measured in the western Sargasso Sea, and crustal aerosol concentrations, sizes, and chemical characteristics were determined at a coastal site near Miami, Florida.

This study has relevance to the Global Backscatter Experiment (GLOBE) and the Laser Atmospheric Wind Sounder (LAWS) activities because it presents a method that can be

[1]Department of Marine Science, University of South Florida, St. Petersburg.
[2]Now at Research and Data Systems, Greenbelt, Maryland.
[3]Marine Research Laboratory, Florida Department of Natural Resources, St. Petersburg.
[4]Rosenstiel School of Marine and Atmospheric Science, University of Miami, Miami, Florida.

Paper number 89JD03280.
0148-0227/91/89JD-03280$05.00

applied to the existing CZCS data set to provide statistics on the spatial and temporal extent of high-backscattering dust particles. Furthermore, the methodology is applicable to future data sets from planned ocean color sensors. Synergistically, the anticipated wind speed and aerosol backscatter data from LAWS will provide information on the height and transport speed of aerosols. These data are valuable to improved interpretation of spectral aerosol radiance imagery from the passive ocean color sensors. Estimates of the flux to the ocean of aeolian aerosols containing such micronutrients as iron are needed to evaluate the potential effect on marine primary productivity [e.g., *Martin and Gordon*, 1988]. Thus Earth-observing system instruments such as the Moderate Resolution Imaging Spectrometer (MODIS), the High Resolution Imaging Spectrometer (HIRIS), and LAWS may together play an important role in providing data to improve such flux calculations.

2. Background and Theory

The Nimbus 7 satellite is in a sun-synchronous orbit at a nominal altitude of 955 km with ascending node (northward crossing of the equatorial plane) near local noon. The CZCS sensor is a scanning radiometer with a ±39° cross-track scan of the six coregistered spectral channels, four in the visible wavelengths (443, 520, 550, and 670 nm), one in the far red (750 nm), and one in the infrared (10.5–12.5 μm) [*Hovis et al.*, 1980]. The sensor has a ground resolution of 825 m at nadir, and the scan mirror can be tilted up to 20° forward or backward along its ground track to reduce specularly reflected sun glint from the sea surface.

The single-component atmospheric correction algorithm is based on quasi-single-scattering theory and the clear-water radiance technique [*Gordon and Clark*, 1981; *Gordon et al.*, 1983*a*]. Single-scattering theory allows radiance arising from Rayleigh scattering (L_r), radiance arising from aerosol scattering (L_a), and water-leaving radiance (L_w) to be separated. The clear-water radiance technique utilizes knowledge of the water-leaving radiance of low-chlorophyll sea water at 520, 550, and 670 nm and knowledge of the radiance due to Rayleigh scattering to determine the radiance due to aerosol scattering by measuring the total radiance received at the sensor (L_t) at each of the wavelengths. The water-leaving radiance at 443 nm (the band most sensitive to chlorophyll absorption) can then be determined through spectral extrapolation to 443 nm of the aerosol radiance. Treatment of the Rayleigh and aerosol scattering in a single-scattering sense (e.g., as independent terms) results in errors in aerosol radiance values less than 10% for aerosol optical thicknesses (τ_a) ≤ 0.6 for scenes unaffected by sunglint [*Gordon et al.*, 1983*a*]. The difference between aerosol radiance calculations made using single-scattering versus multiple-scattering methods increases with aerosol optical thickness, observational zenith angle, and, to a lesser extent, solar zenith angle. However, for aerosol optical thicknesses (τ_a) ≤ 0.6, *Gordon and Castano* [1989] demonstrated that for a wide variety of aerosol types, this difference is linear with L_a and can be determined within 5–8% except at the edges of the CZCS scan. Thus given knowledge of the scan mirror forward tilt angle (e.g., 0° or +20°) and the cross-track scan angle, multiple-scattering estimates of aerosol radiance can be determined from single-scattering calculations of aerosol radiance.

Using the notation and arguments of *Gordon et al.* [1983*a*] and single-scattering theory, the total radiance $L_t(\lambda)$ received at the satellite can be divided into its components: the radiance values arising from Rayleigh scattering $L_r(\lambda)$, the contribution arising from $L_a(\lambda)$, and the water-leaving radiance $L_w(\lambda)$ diffusely transmitted to the top of the atmosphere $L_w(\lambda)t(\lambda)$ [*Gordon*, 1978; *Tanre et al.*, 1979; *Gordon et al.*, 1983*a*]:

$$L_t(\lambda) = L_r(\lambda) + L_a(\lambda) + L_w(\lambda)t(\lambda) \quad (1)$$

Gordon [1978] showed, through comparisons with "exact" multiple-scattering calculations using a number of likely aerosol models, that multiple-scattering effects from the ocean to the satellite could be neglected with an error of about 3% if attenuation of the path radiance was ignored. Note that these path radiance values observed at the satellite implicitly include effects due to ozone absorption.

The contribution of $L_r(\lambda)$ due to Rayleigh scattering can be determined a priori from the sun and spacecraft zenith angles. The diffuse transmittance of the atmosphere, $t(\lambda)$, is considered to be known, since it is primarily a function of Rayleigh and ozone optical thicknesses (τ_r and τ_{0z}) and the satellite zenith angle (θ) and is only secondarily a function of aerosol attenuation, which is dominated by near-forward scattering [*Tanre et al.*, 1979; *Gordon and Clark*, 1981; *Gordon et al.*, 1983*a*]. This leaves $L_a(\lambda)$ and $L_w(\lambda)$ as the only unknowns in the equation.

The solution to equation (1) is effected by deriving an expression for the ratio of aerosol radiances in CZCS channels 1, 2, and 3 to channel 4, where subscripts denote the channel number and correspond to λ at 443, 520, 550, and 670 nm, respectively.

$$L_a(\lambda_i)/L_a(\lambda_4) = \varepsilon(\lambda_i, \lambda_4)[F_0'(\lambda_i)/F_0'(\lambda_4)] \quad (2)$$

where

$$\varepsilon(\lambda_i, \lambda_4) = \frac{\omega_a(\lambda_i)\tau_a(\lambda_i)p_a(\theta, \theta_0, \lambda_i)}{\omega_a(\lambda_4)\tau_a(\lambda_4)p_a(\theta, \theta_0, \lambda_4)} \quad (3)$$

Here, $\omega_a(\lambda_i)$ is the single-scattering albedo of the aerosol (assumed for marine aerosols to be 1.0), $\tau_a(\lambda_i)$ the aerosol optical thickness, and $p_a(\Theta, \Theta_0, \lambda_i)$ is the aerosol phase function. For nonabsorbing aerosols, $\varepsilon(\lambda_i, \lambda_4)$ is a term dominated by the aerosol optical thickness, since phase functions for most likely aerosol models at CZCS observational angles relative to the sun are only weakly dependent upon wavelength [*Gordon*, 1978; *Gordon and Clark*, 1981; *Gordon et al.*, 1983*a*]. The Θ and Θ_0 are the zenith angles of a pixel to the satellite and sun, respectively. $F_0'(\lambda)$ in equation (2) is the extraterrestrial solar irradiance corrected for absorption by an ozone layer of optical thickness τ_{0z}.

Now, (1) may be expressed as

$$L_t(\lambda_i) - L_r(\lambda_i) - t(\lambda_i)L_w(\lambda_i) = L_a(\lambda_i)$$

$$= S(\lambda_i, \lambda_4)[L_t(\lambda_4) - L_r(\lambda_4) - t(\lambda_4)L_w(\lambda_4)] \quad (4)$$

where

$$S(\lambda_i, \lambda_4) = \varepsilon(\lambda_i, \lambda_4)[F_0'(\lambda_i)/F_0'(\lambda_4)] \quad (5)$$

The clear-water radiance theory [*Gordon and Clark*, 1981] is now invoked to determine $L_a(\lambda_i)$ in (4) for each pixel in a small, clear-water region. The epsilon values derived for

spectral bands 2, 3, and 4 using (5) are spatially averaged and used to "type" the aerosol. The basis for the theory is that where chlorophyll *a* plus phaeophytin *a* concentrations $\langle C \rangle$ are less than 0.25 mg/m^3, the normalized water-leaving radiance $\{L_w(\lambda_i)\}$ at 520, 550, and 670 nm can be designated a priori, within 10%, to be 0.498, 0.30, and <0.015 mW/cm^2/μm/sr, respectively, for the CZCS [*Gordon and Clark*, 1981; *Gordon et al.*, 1983*a*]. For a given wavelength, $L_w(\lambda_i)$ can be related to $\{L_w(\lambda_i)\}$ through

$$L_w(\lambda_i) = \{L_w(\lambda_i)\}t(\theta_0, \lambda_i)\mu_0 \tag{6}$$

where $\mu_0 = \cos \theta_0$, and [*Gordon and Clark*, 1981]

$$t(\lambda) = \exp\{-[\tau_r(\lambda)/2 + \tau_{0z}(\lambda) + (1 - \omega_a(\lambda)F)\tau_a(\lambda)]/\mu_0\} \tag{7}$$

F is the probability that a photon scattered by an aerosol is directed in a forward direction, and the term $(1 - \omega_a F)\tau_a$ is generally unknown. For typical aerosol models, however, $(1 - \omega_a F) < 1/6$, so for $\tau_a \leq 0.6$ the entire term can be ignored with an error in $t(\lambda)$ of less than 10% for small solar zenith angles [*Gordon and Clark*, 1981]. Thus $\varepsilon(520, 670)$, $\varepsilon(550, 670)$, and $\varepsilon(670, 670)$ can be determined over clear water and then applied to regions where $\langle C \rangle$ is greater than 0.25 mg/m^3. It should be noted that while the aerosol type is fixed by this method, the aerosol concentration may vary.

$\varepsilon(443, 670)$ is determined by a power function [*Angstrom*, 1964; *Gordon and Clark*, 1981] with Angstrom exponent $\eta(\lambda_i)$:

$$\varepsilon(\lambda_i, \lambda_4) = (\lambda_i/\lambda_4)^{\eta(\lambda_i)} \tag{8}$$

and $\eta(\lambda_1)$ is the spectral average of $\eta(\lambda_2)$ and $\eta(\lambda_3)$. This method is usually applied to a 5 × 5 pixel region of a clear-water portion of the scene in order to characterize the spectral nature of the scattering by the aerosol "type" associated with that region. The derived epsilon values are then assumed invariant over the entire scene [see *Gordon et al.*, 1983*a*]. The "type" of aerosol is thus assumed constant for the entire scene, but the concentration can vary as observed using $L_a(670)$, since at this wavelength, $L_w(670) \approx 0$. The aerosol can also be "typed" pixel by pixel for the entire scene if no region in the scene has $\langle C \rangle \geq 0.25$ mg/m^3. This approach is computationally quite expensive, however, and is rarely used.

Chlorophyll *a* plus phaeophytin *a* concentrations $\langle C \rangle$ are then determined from the water-leaving radiances by regression equations of the form [*Gordon et al.*, 1983*a*]

$$\langle C \rangle = A[L_w(\lambda_i)/L_w(550)]^B \tag{9}$$

We introduce the two-component method, which simultaneously determines the aerosol radiances of two widely different aerosols present in the same clear-water scene. The method follows the single-component model up through (5). However, instead of determining an $\varepsilon(\lambda_i, \lambda_4)$ value for a single aerosol type and applying it to the entire scene, $\varepsilon_j(\lambda_i, \lambda_4)$ values are determined for each of two aerosol types. The method works best if there are different portions of the scene where each aerosol type dominates and can be characterized independently, even though much of the scene contains mixtures of the two types. Thus the aerosol "typing" is of an operational rather than theoretical nature unless additional knowledge of the aerosol spectral characteristics is available.

The $S_j(\lambda_i, \lambda_4)$ values corresponding to the $\varepsilon_j(\lambda_i, \lambda_4)$ values are then calculated by (5) pixel by pixel and placed into a 2 × 3 matrix to determine the aerosol radiances for each component, $L_{aj}(670)$, $j = 1, 2$:

$$\begin{bmatrix} S_1(520, 670) & S_2(520, 670) \\ S_1(550, 670) & S_2(550, 670) \\ 1 & 1 \end{bmatrix} \begin{bmatrix} L_{a_1}(670) \\ L_{a_2}(670) \end{bmatrix} = \begin{bmatrix} L_a(520) \\ L_a(550) \\ L_a(670) \end{bmatrix} \tag{10}$$

$L_{a1}(670)$ and $L_{a2}(670)$ are the radiances at 670 nm for aerosol types 1 and 2. Each row of the coefficient matrix represents a particular wavelength, while the columns represent the two aerosol types. The method applies only to low chlorophyll waters where $L_w(\lambda_i)$ can be specified for $i = 2, 3, 4$. $\varepsilon_j(\lambda_i, \lambda_4)$ values are determined by selecting regions in the scene where the aerosols are predominantly of one type and individually determinable by the clear-water method of *Gordon and Clark* [1981]. Thus the only unknowns in (10) are $L_{aj}(670)$ values. The resulting problem is an overdetermined system (10), which is solved by a least squares method using QR factorization [*Strang*, 1986]. Solution of (10) provides the contribution $L_{aj}(670)$ of each aerosol type to the aerosol radiance at 670 nm.

The radiance contribution of each aerosol type to the total aerosol radiance observed in the blue channel is estimated as

$$L_a(443) = S_1(443, 670)L_{a_1}(670) + S_2(443, 670)L_{a_2}(670) \tag{11}$$

The chlorophyll pigment concentration $\langle C \rangle$ is determined by solving (4) for $L_w(433)$ and $L_w(550)$ and substituting in [*Gordon et al.*, 1983*a*]

$$\langle C \rangle = 1.13[L_w(443)/L_w(550)]^{-1.71} \tag{12}$$

3. Methods

Calibrated radiance and temperature tapes (CRTT) for five sufficiently cloud free CZCS images in late June 1980 were obtained from NASA for processing and comparison with ship and coastal data collected when a major Saharan dust event was observed over southern Florida [*Carder et al.*, 1986]. These tapes were processed using the Florida Department of Natural Resources Marine Resource Geobased Information System (Gould Concept 32/27 with Comtal display and ELAS applications software). Processing of the imagery was carried out using the revised sensor calibration values for Gain 1 and the revised F_0 values from Table IV of *Gordon et al.* [1983*a*]. The sensor calibration equation provided by *Gordon et al.* [1983*b*] was used to adjust CZCS calibration as a function of orbit number (time). Spacecraft position and orientation data were provided directly on the CRTTs.

4. Results and Discussion

On June 19 and 20, 1980, a major influx of Saharan dust into the western Sargasso Sea was recorded at 25°59′N latitude, 75°59′W longitude in holographic microscopy samples of the surface waters and in sediment trap data from 30-m depth [*Carder et al.*, 1982, 1986]. The main pulse of the dust did not begin to arrive at Miami, Florida, until approximately 3 days later. Surface winds for the region were generally weak and from the south, with a more easterly and

TABLE 1. Values for Elements $\epsilon_j(\lambda_i, \lambda_4)$ for Bluish Aerosols and Saharan Dust for CZCS Orbits in June 1980

	λ, nm	Bluish Aerosol	Saharan Dust
Orbit 8326	443	2.067	0.989
June 17, 1980	520	1.682	1.033
	550	1.330	0.961
	670	1	1
Orbit 8381	443	1.364	0.952
June 21, 1980	520	1.245	1.013
	550	1.130	0.940
	670	1	1
Orbit 8464	443	1.482	0.987
June 27, 1980	520	1.394	1.026
	550	1.119	0.964
	670	1	1
Orbit 8478	443	1.732	0.943
June 28, 1980	520	1.470	1.002
	550	1.246	0.940
	670	1	1
Orbit 8492	443	1.655	0.968
June 29, 1980	520	1.429	1.018
	550	1.185	0.951
	670	1	1

southeasterly component for the upper level winds in the eastern extreme of the study region [*Carder et al.*, 1986].

CZCS imagery for orbit 8326 (June 17, 1980) covering the Florida Straits and western Sargasso Sea is shown in Plate 1. Plate 1 is the color-enhanced, atmospherically uncorrected subscene of orbit 8326, showing Palm Beach, Florida, on the western edge. A strong aerosol gradient is apparent along the eastern edge of Plate 1. The area corresponds to the approximate position of the influx of Saharan dust on this date [*Carder et al.*, 1986]. Analysis of spectral reflectances of Saharan dust captured on filter pads indicated that such aerosols backscattered strongly in the red wavelengths [*Patterson*, 1981; *Prospero and Carlson*, 1972], in contrast to the white-scattering marine aerosols and blue-scattering hazes that were likely present in portions of the scene.

Table 1 contains $\epsilon_j(\lambda_i, \lambda_4)$ values used in the two-component aerosol model (equations 10 and 11)) for the five scenes in late June 1980. Aerosol type 1 (column 2, Table 1) has $\epsilon_j(\lambda_i, \lambda_4)$ values greater than 1.0, typical of fine hazelike aerosols. It was derived using the single-component clear-water method [*Gordon and Clark*, 1981] from the imagery just to the east of the Bahamas in Plate 1 for orbit 8326 and from high $\epsilon_j(\lambda_i, \lambda_4)$ regions for the other images. A mean of $\epsilon_j(\lambda_i, \lambda_4)$ values from 5 × 5 pixel areas was used to minimize the effect of noise. Aerosol type 2 has epsilon values of <1.0, which would be expected for blue-absorbing aerosols such as Saharan dust. The Saharan $\epsilon_j(\lambda_i, \lambda_4)$ values were derived from regions of low $\epsilon_j(\lambda_i, \lambda_4)$ and relatively high $L_a(670)$ for each scene. Care was taken to avoid the eastern and western edges of the scenes because the validity of the single-scattering assumption decreases at the limbs of the CZCS scan [see *Hovis et al.*, 1980; *Gordon and Castano*, 1987].

Saharan Aerosol Radiance Variations

Five sufficiently cloud free CZCS images were atmospherically corrected by the two-component method to generate a sequence of Saharan dust aerosol radiance images at 670 nm ($L_a(670)$). The part of the sequence from June 27 to 29, 1980, clearly shows the movement of the Saharan dust over Florida (yellow-red patches in Plate 2). The dust was centered over the Bahamas by June 27 and just west of south Florida on June 28. By June 29 it was centered over the Yucatan Channel and the Loop Current region of the southeastern Gulf of Mexico.

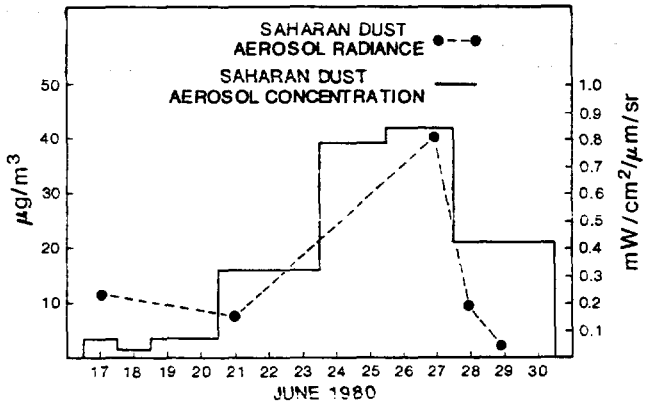

Fig. 1. Comparison of aerosol mass concentration data (2- and 3-day means) from a coastal aerosol collection tower with instantaneous aerosol radiance values for Saharan dust over adjacent waters in the Florida Straits.

A 25 × 25 pixel area was selected in the Florida Straits near the coastal, aerosol-filtration site (see small box in Plate 2a) in order to quantify the movement of the Saharan dust over Florida. The time series of dust aerosol radiances corrected for slant-path length is compared for this site with observed aerosol concentrations collected nearby at the University of Miami (Figure 1). These results suggest a covariation between Saharan dust radiance and Saharan dust concentration and demonstrate the ability of the two-component algorithm to identify and monitor blue-absorbing aerosols.

The maximum desert aerosol radiance value progressed westward with time (Plate 2), but the maxima changed little from June 27 to June 29. The desert aerosol radiance values near Miami (Figure 1) decreased markedly after June 27, however, but the aerosol concentration at the base of the air column decreased more gradually with time. This suggests that most of the residual desert aerosols in the air column on June 28 and 29 were in the lower part of the atmosphere where they were available for filtration.

The Saharan aerosol radiance values off Miami from June 17 were likely enriched by anthropogenic aerosols from the Miami area, since the surface winds were from the southwest at that time [*Carder et al.*, 1986]. Such yellowish hazes would be spectrally more similar to Saharan dust than to the blue-rich aerosol haze (see $\epsilon_j(\lambda_i, \lambda_4)$ values in Table 1) derived from the region northeast of the Bahamas.

The improved correspondence between surface measures of aerosol mass concentration and Saharan aerosol radiance between June 21 and 27 indicates that dust in the marine boundary layer generally covaried with the total column aerosol radiance and that the size distribution was not rapidly changing. It also suggests that between June 21 and 29, the desert aerosol radiance dominated the contributions to total radiance measured at the satellite.

Plate 1. An atmospherically uncorrected subscene of CZCS orbit 8326, June 17, 1980. The red shading indicates Saharan dust (eastern edge), blue indicates bluish haze (center), and yellow-brown indicates coastal aerosols and chlorophyll pigments (Florida Straits). Continuous lines show latitude and longitude.

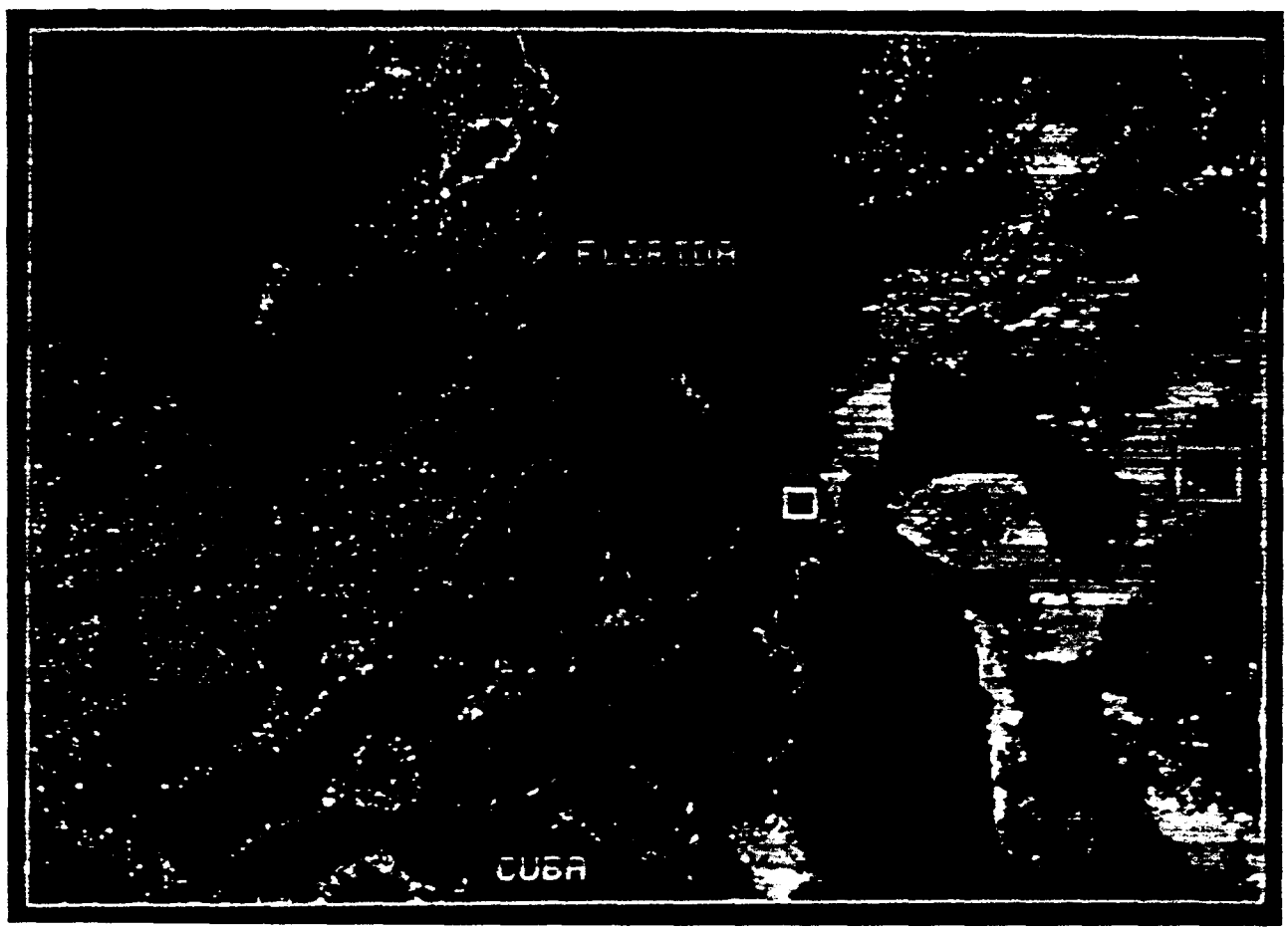

Plate 2*a*

Plate 2. Time series over Florida of aerosol radiance $L_a(670)$ due to Saharan dust on (*a*) June 27, 1980, (*b*) June 28, 1980, and (*c*) June 29, 1980. Red and yellow shading in each frame indicates the main dust pulse as inferred from the dust aerosol radiances. The color table indicates Saharan dust aerosol radiance values (mW cm^{-2} μm/sr). Bright regions (clouds, land, and shoal areas) are masked in black.

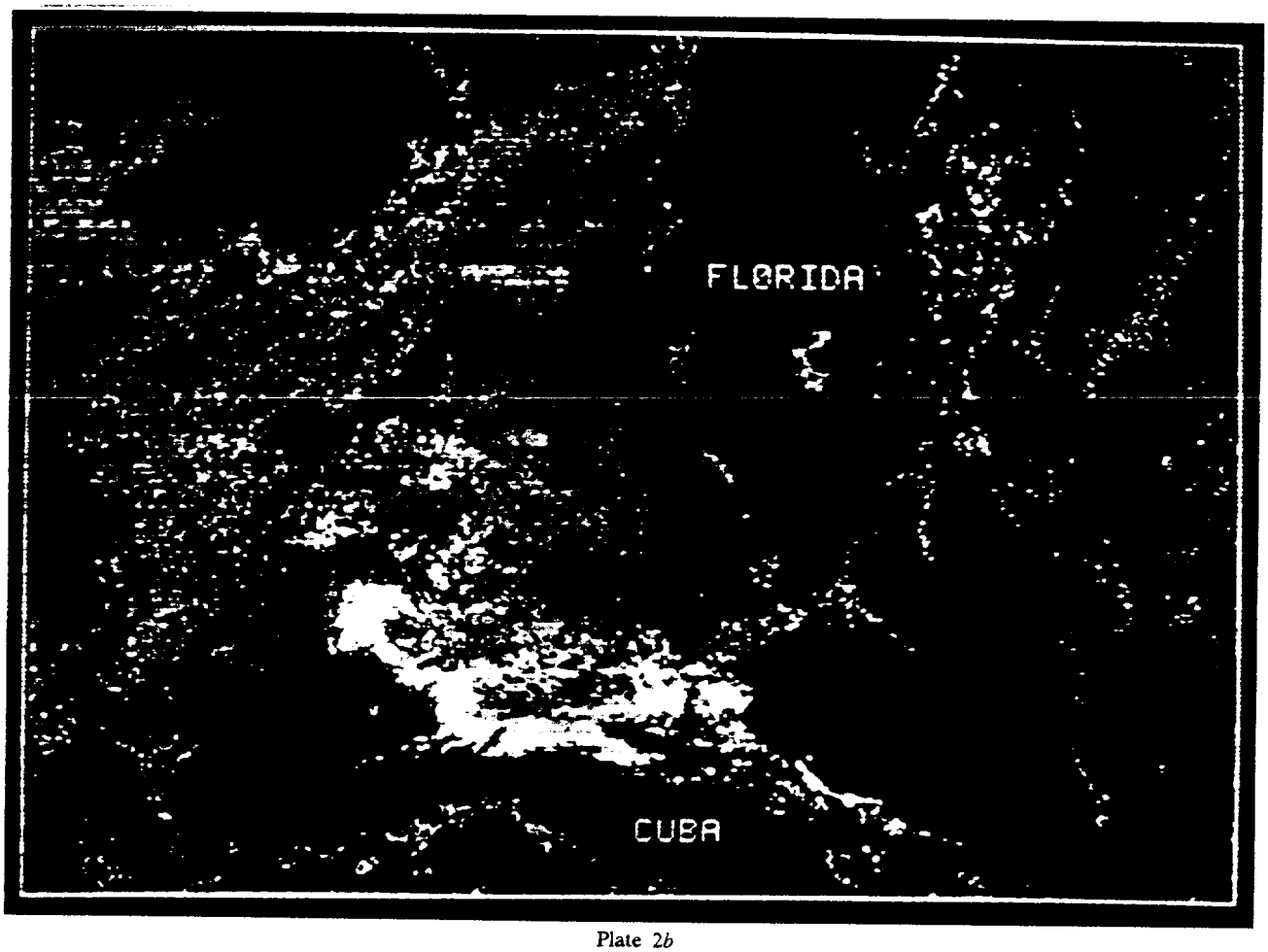

Plate 2*b*

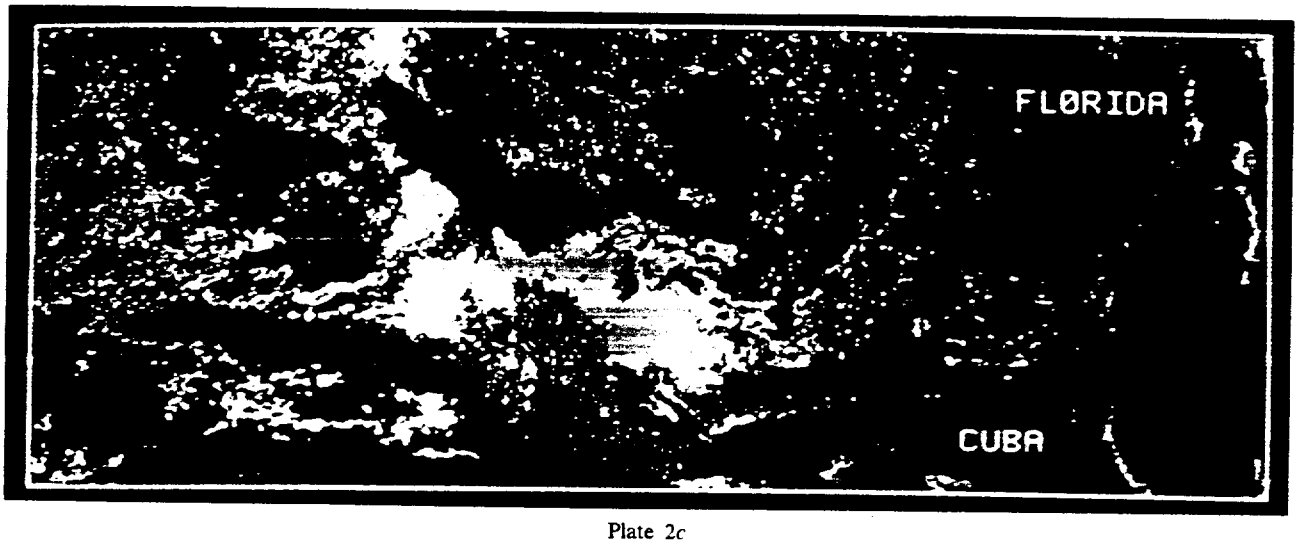

Plate 2*c*

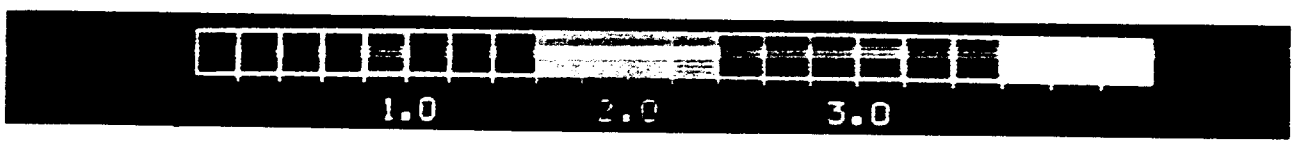

Plate 2. (continued)

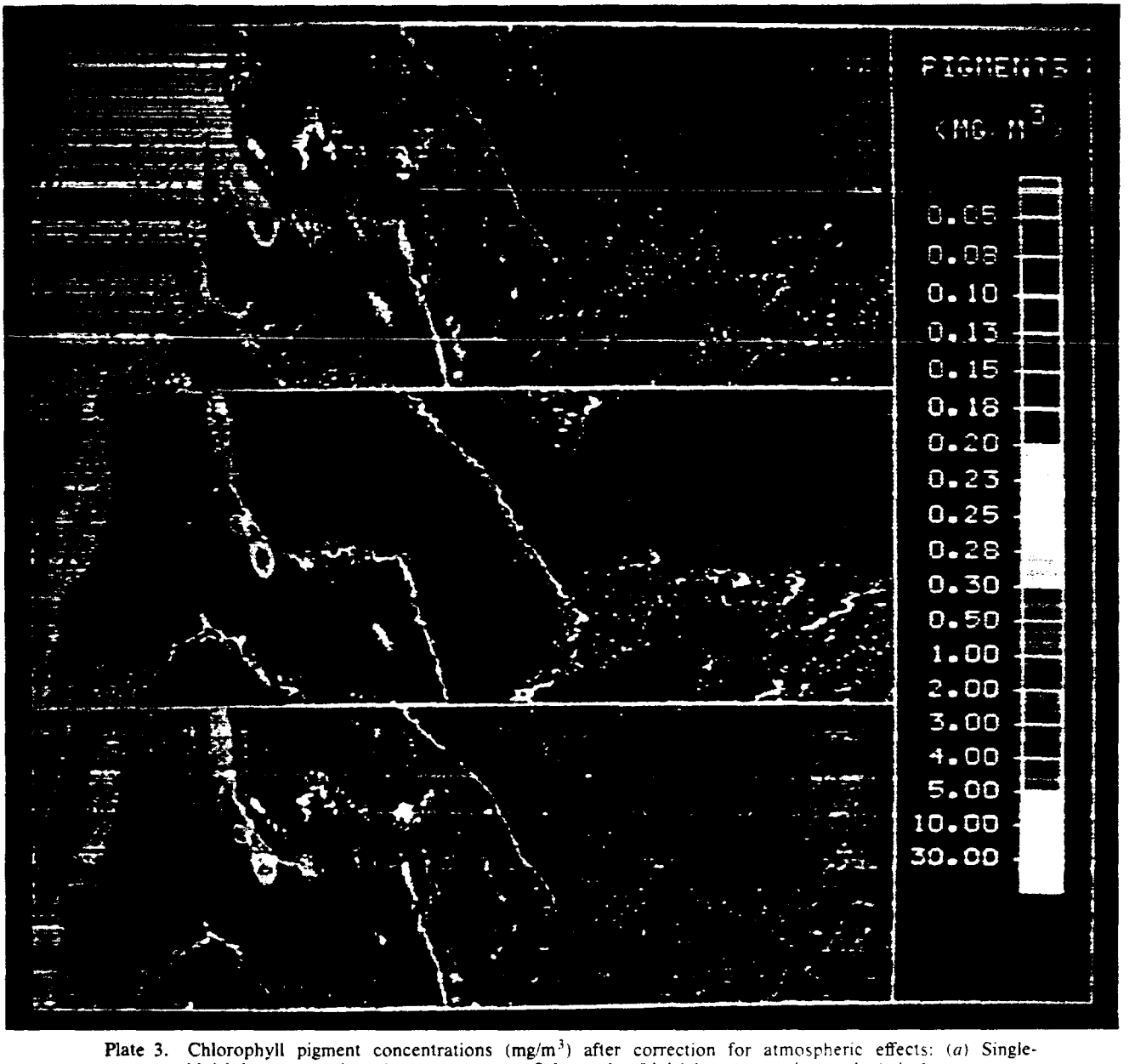

Plate 3. Chlorophyll pigment concentrations (mg/m^3) after correction for atmospheric effects: (*a*) Single-component, bluish-haze correction, (*b*) two-component Saharan dust/bluish haze correction, and (*c*) single-component, anthropogenic aerosol correction.

Carder et al. [1986] showed that the leading edge of the dust reaching Miami on June 21–23 was large-particle-rich and heavy-mineral-rich compared to the trailing edge of June 27–30. This would indicate that the lead edge of the dust plume should have a lower ratio of dust radiance to unit mass concentration, since the light scattered is proportional to the cross-sectional area for particles which are large relative to the wavelength of light [*Van de Hulst*, 1957] and mass is proportional to the particle volume.

This expectation is confirmed by the radiance/mass ratios: 0.073–0.09 (kW km)/(g μm sr) for June 21 (depending upon whether the nondust aerosol background mass concentration was 0 or 4 μg/m^3) and 0.20 (kW km)/(g μm sr) for June 27. However, if other confounding factors such as variation in the vertical distribution of dust were of only minor importance during this time span, the factor of 2 variation in the radiance-to-mass ratio suggests that the aerosols at the leading edge were roughly twice the diameter of the aerosols at the trailing edge. Mass concentration data of *Carder et al.* [1986] show mode values of 2.5–5.0 μm in diameter for both heavy mineral and non-heavy mineral classes for June 20–23, and modes of 0.5–1.0 μm and 1.0–2.5 μm in diameter for the heavy and non-heavy mineral classes, respectively, for June 25–27. This size change is quite close to that required to explain changes in the radiance-to-mass ratios.

Care must be taken, however, in interpreting total column, single-scattering aerosol radiance values in terms of aerosol concentrations measured at the base of the column. Vertical inhomogeneities in aerosol concentration and type, changes in particle size and specific gravity distributions with time, and variations in the applicability of single-scattering theory with aerosol type, optical thickness, and viewing geometry all contribute uncertainty to any interpretation.

Gordon and Castaño [1989] recently demonstrated for a

TABLE 2. Comparison of in Situ Chlorophyll *a* Plus Phaeophytin *a*, ⟨*C*⟩

	⟨*C*⟩, mg/m³			
Station	In Situ	One-Component Anthropogenic	One-Component Bluish Aerosol	Two-Component Method
1: 25°55′N, 76°00′W	0.045 ± 0.014	0.108 ± 0.013	0.126 ± 0.015	0.080 ± 0.009
2: 26°15′27″N, 79°20′30″W	0.09	0.139 ± 0.021	0.200 ± 0.026	0.148 ± 0.013

Values are determined from CZCS orbit 8326 using the two-component method and the single-component method for each of two different aerosol types.

wide variety of aerosol types that the single-scattering approximation of aerosol radiance (used here) varies linearly with "exact," multiple-scattering calculations of aerosol radiance. The linear relationship is primarily a function of the scan angle for a given mirror tilt (20° in our case). According to their analyses, then, the Saharan aerosol radiance values for June 21 and 27 (Figure 1) are about 5–7% lower than the true, multiple-scattering values would be, and those for June 17 and 28 are about 15–25% too low. Such adjustments to Figure 1 to better simulate true multiple-scattering aerosol radiance values would actually improve the correspondence between the time series sequences for Saharan dust aerosol radiance and concentration.

Chlorophyll Concentrations

Consistency of CZCS-derived chlorophyll determinations before, during, and after Saharan dust passage are observed as an indirect test of the two-component algorithm. After removal of the atmospheric radiance, equation (12) was applied to the water-leaving radiance imagery to derive the pigment concentration ⟨*C*⟩ for June 17, 1980 (orbit 8326) (see Plate 3), for which in situ chlorophyll values were available. Plate 3*a* shows pigment concentrations resulting from application of the single-component atmospheric correction method. The $\varepsilon_j(\lambda_i, \lambda_4)$ values were derived using the clear-water technique for pixels in an area northeast of the Bahamas which was dominated by a bluish haze (hereafter referred to as the bluish-aerosol method). Plate 3*b* shows the results of the two-component method. Plate 3*c* shows the results of the single-aerosol method using a clear-water pixel region in the Florida Straits area near Palm Beach, where haze from the adjacent metropolitan area appears to have been transported by weak southwesterly winds. This will be referred to as the anthropogenic aerosol method.

Comparing this imagery to the total radiance imagery of Plate 1 suggests that pigments in Plate 3*a* covary with the reddish aerosols in the northeastern portion of the scene and with the anthropogenic aerosols in the Florida Straits near Miami. The two-component method produced a quite uniform chlorophyll field in the Sargasso Sea as one would expect, with no evidence of covariance with the aerosols apparent in Plate 1. The anthropogenic method produces a chlorophyll field much closer to the two-component field except under the reddish aerosols at the eastern and southeastern portions of the image.

In situ chlorophyll measurements are available for the period June 17–21, 1980. Comparison of these measurements with those from 11 × 11 pixel areas from orbit 8326 illustrates the relative accuracies of the methods in determining chlorophyll *a* plus phaeopigments *a* ⟨*C*⟩ for different locations in the scene (Table 2). The locations of the in situ measurements are also identified in Table 2 and can be geolocated using Plate 1. Three of the in situ measurements were made in regions covered by clouds in orbit 8326, so a mean of these values was taken and compared to the nearest cloud-free 11 × 11 pixel area (hereafter referred to as station 1). A significant anomaly in the CZCS-derived pigments due to cloud saturation is typically manifest on the east side of clouds in CZCS data [*Mueller*, 1988]. To avoid these areas, we selected 11 × 11 pixel areas that were east of any visible saturation effect, at least 10 pixels on the downscan side of clouds, and maintained a border of at least one pixel to the north, south, and west sides of clouds. The other site (station 2) was in the Florida Straits.

The measured chlorophyll values are lower than CZCS-derived values using either the single- or the two-component methods (Table 2). The two-component method overestimates the chlorophyll concentration by 64–78%, while the single-component method overestimates the chlorophyll concentration by 54–140% (anthropogenic aerosol) and by 122–180% (bluish aerosol). The performance of the single-component anthropogenic method improved when the region observed was covered by an aerosol with epsilons that were similar in type to the anthropogenic epsilon values (e.g. in the Florida Straits). There were no in situ chlorophyll stations in an area covered with bluish aerosols, such as northeast of Grand Bahamas Island. As a result, tests of chlorophyll retrievals using the bluish aerosol, single-component method under ideal conditions were not possible.

The two-component method provided consistent results, and in addition, its performance was independent of location and of aerosol type(s). It provided results nearly as good as those of the single-component method specifically calibrated through epsilon selection for the study or comparison area, and its use did not manifest the severe deterioration in performance exhibited by single-component methodologies applied to regions containing aerosols with epsilon values dissimilar to those of the calibration area.

To check for scene-to-scene consistency of chlorophyll values as the Saharan dust cloud moved across the Sargasso Sea, a 51 × 51 pixel region northeast of Grand Bahamas Island (large box in Plate 2*a*) was monitored from June 17 to 28, 1980, using the two-component method. Table 3 shows mean chlorophyll values of 0.0875 ± 0.005 mg/m³ (constant within 6%) for that period, even though the aerosols varied from bluish, hazelike epsilons on June 17, to reddish Saharan dustlike epsilons on June 27. During this period, Saharan aerosol radiance values ranged from 0.0716 to 1.1458 mW/cm²/μm/sr. This clear-water region was not in the field of view of the CZCS on June 29.

TABLE 3. Time Series of Chlorophyll *a* Plus Phaeophytin *a* Concentrations Before, During, and After a Saharan Dust Event

Date (Orbit)	Saharan Dust Aerosol Radiance, mW/cm^2/μm/sr	Pigment, mg/m^3
June 17, 1980 (8326)	0.0716 ± 0.04085	0.078 ± 0.0066
June 21, 1980 (8381)	0.9258 ± 0.17065	0.099 ± 0.0084
June 27, 1980 (8464)	1.1458 ± 0.10426	0.088 ± 0.0071
June 28, 1980 (8478)	0.3283 ± 0.25879	0.085 ± 0.0074

Concurrent aerosol radiances at 670 nm determined from the same subscene are also shown. Mean values for a 51 × 51 pixel subregion of the Sargasso Sea are listed.

The lowest chlorophyll *a* plus phaeophytin *a* values measured for the northern Sargasso Sea and Gulf Stream during a CZCS validation cruise in June 1979 were 0.05–0.09 mg/m^3 [*Gordon et al.*, 1983*b*], values consistent with our measured values of 0.045 and 0.09 mg/m^3. The upper end of this range is also consistent with our 4-day mean value of 0.0875 mg/m^3 which was determined by the two-component method northeast of the Bahamas, a region expected to contain waters with very low chlorophyll pigment values. Thus it appears that the CZCS-derived values of Tables 2 and 3 are biased high by about 0.04 mg/m^3. To estimate the decay in radiometric sensitivity for the CZCS blue channel, *Gordon et al.* [1983*b*] assumed that the lowest summer chlorophyll *a* plus phaeophytin *a* values for the Sargasso Sea region was about 0.09 mg/m^3. A pigment estimate was required for the imagery used in these analyses in order to estimate water-leaving radiance values for this pigment-sensitive band. This conservative selection is about 0.04 mg/m^3 higher than the lowest values measured both in summer 1979 and in summer 1980. This assumed value also turns out to be very close to our derived mean value (Table 3). It is possible that by using, as we did, the *Gordon et al.* [1983*b*] calibration values derived from their study of the sensitivity decay of CZCS blue channel, we have been limited to retrievals for $\langle C \rangle$ that are no lower than top end of the 0.05- to 0.09-mg/m^3 range expected for the Sargasso Sea during the summer. This may explain at least some of the overestimation in $\langle C \rangle$ observed using single- and two-component aerosol radiance methodologies in determining chlorophyll concentrations for the Sargasso Sea.

The two-component method appears to have spectrally separated Saharan dust radiance contributions to the total aerosol radiance detected with the CZCS from those due to a bluish haze always present in the low-wind scenes that were investigated. The spectral characteristics of these two aerosol components were quite distinct (Table 1), which must have aided in the spectral classification process. The surface winds were very light during most of this period, suggesting that large-diameter, whitish marine aerosols were likely not providing a significant scattering contribution to the aerosol radiance during the study. The epsilon values expected for such aerosols would be close to 1.0, so it is possible that during periods of high wind the aerosol radiance due to large marine aerosols could be classified by the technique as "Saharan dust." Such a misclassification would be less likely for Saharan dust found much closer to its source, however, since very "red" epsilon values of as low as 0.3–0.4 have been observed over the Atlantic off the coast of north Africa (A. Morel, personal communication, 1989). The form of the spectral extrapolation function for such strongly absorbing aerosols would likely require a change from an Angstrom exponential form (equation (8)) to some other form. A linear form is suggested by the linear decrease with wavelength (from 430 nm to 620 nm) of the imaginary part of the index of refraction for Saharan dust captured on filter pads [see *Patterson*, 1981].

5. Conclusions

During the latter half of June 1980 a major influx of Saharan dust passed over the western Sargasso Sea and the southern part of the Florida peninsula. During much of this period of time, CZCS imagery exhibited sharply defined frontal boundary features in the atmosphere, with a bluish, hazelike character on one side and a slightly reddish, turbid appearance on the other. To smoothly remove atmospheric radiance effects in order to view the ocean without a significant residual atmospheric signature in the water-leaving radiance field, a method was required to remove aerosol radiance effects due to more than a single aerosol component or type.

A two-component method for spectrally separating Saharan dust and bluish haze contributions to the total aerosol radiance was developed and applied, resulting in dust aerosol radiances that were consistent as a function of time with the dust concentration and size changes observed at a nearby field station. Furthermore, covariance between chlorophyll and aerosol radiance fields was not evident in the imagery. As a result, chlorophyll pigment (chlorophyll *a* plus phaeophytin *a*) concentration values extracted by the two-component technique were stable (0.0875 ± 0.005 mg/m^3) over time for a region of the Sargasso Sea over which the aerosol radiance values changed from those characteristic of a bluish haze to those of a turbid, reddish dust. With this method the CZCS-derived chlorophyll values for this region were consistent with CZCS-derived and field values for the clearest waters of the northern Sargasso reported for the prior year (0.05–0.09 mg/m^3) but were some 64–78% higher than synoptically measured values.

The chlorophyll pigment values determined using a single-aerosol, CZCS method overestimated chlorophyll pigment concentrations by 54–180%, depending upon the aerosol type in the portion of the scene under comparison. For epsilon values (aerosol types) consistent with the aerosol resident in the study area the single-component method performed as well as did the two-component method. However, for regions with mixed aerosol types, or epsilons no longer consistent with the resident aerosol, the single-component method delivered values that were no longer consistent with either historical or measured numbers. While the two-component method provided relatively stable chlorophyll pigment values which were insensitive to the aerosol type resident in the region, the 50–80% enrichment or high bias apparent for both methods may be attributable to an assumption used in estimating the reduction of sensitivity for the blue channel of the CZCS with time since launch: that the chlorophyll pigments for the clearest part of the northern Sargasso Sea were 0.09 mg/m^3. This number is very close to the value derived from the two-component method. The blue channel plays no role in the derivation of aerosol spectral

characteristics or epsilon values using the clear-water radiance methodology, so the chlorophyll assumption listed above had no effect on any of the aerosol radiance values reported.

Since aerosol radiance is a characteristic of the total air column, it provides a different kind of information than is provided by single-point aerosol measurements (aircraft or ground station). Passive spectral radiometry from satellites provides broad and repeat coverage that can complement data provided by both the GLOBE and LAWS missions, especially if the source of each general spectral type of aerosol in the scene can be inferred from ancillary information. GLOBE and future LAWS data will reveal the vertical structure of backscattering by the larger particles, and CZCS, Sea-WiFS, MODIS, and HIRIS data can provide the spectral character of the total column backscattering, suggesting probable aerosol types and possible sources for them. Horizontal and vertical aerosol fluxes may ultimately be estimated from contemporaneous and sequential MODIS and LAWS imagery combined with aircraft and ground station sampling of aerosol size and composition.

Acknowledgments. Special thanks to Peter Ortner (NOAA/AOML), who provided chlorophyll *a* and phaeophytin *a* values for comparison to the satellite imagery. This work was supported under NASA grant NAGW-465 and NSF grant OCE-85-00739 to the University of South Florida and under NSF grants ATM-8016127 and ATM-8209759 to the University of Miami.

REFERENCES

Angstrom, A., The parameters of atmospheric turbidity, *Tellus*, *16*, 64, 1964.

Carder, K. L., R. G. Steward, and P. R. Betzer, In situ holographic measurements of the sizes and settling rates of oceanic particulates, *J. Geophys. Res.*, *87*, 5681–5685, 1982.

Carder, K. L., R. G. Steward, P. R. Betzer, D. L. Johnson, and J. M. Prospero, Dynamics and composition of particles from an aeolian input event to the Sargasso Sea, *J. Geophys. Res.*, *91*, 1055–1066, 1986.

Gordon, H. R., Removal of atmospheric effects from satellite imagery of the oceans, *Appl. Opt.*, *17*, 1631–1636, 1978.

Gordon, H. R., and D. J. Castano, Coastal zone color scanner atmospheric correction algorithm: multiple scattering effects. *Appl. Opt.*, *26*, 2111–2122, 1987.

Gordon, H. R., and D. J. Castano, Aerosol analysis with the coastal zone color scanner: A simple method for including multiple scattering effects, *Appl. Opt.*, *28*, 1320–1326, 1989.

Gordon, H. R., and D. K. Clark, Clear water radiances for atmospheric correction of coastal zone color scanner imagery, *Appl. Opt.*, *20*, 4175–4180, 1981.

Gordon, H. R., D. K. Clark, J. W. Brown, O. B. Brown, R. H. Evans, and W. W. Broenkow, Phytoplankton pigment concentrations in the Middle Atlantic Bight: Comparison of ship determinations and CZCS estimates, *Appl. Opt.*, *22*, 20–36, 1983*a*.

Gordon, H. R., J. W. Brown, O. B. Brown, R. H. Evans, and D. K. Clark, Nimbus 7 CZCS: Reduction of its radiometric sensitivity with time, *Appl. Opt.*, *22*, 3929–3931, 1983*b*.

Hovis, W. A., et al., Nimbus-7 coastal zone color scanner: System description and initial imagery, *Science*, *210*, 60–63, 1980.

Martin, J. H., and R. M. Gordon, Northeast Pacific iron distribution in relation to phytoplankton productivity, *Deep Sea Res.*, *35*, 177–196, 1988.

Mueller, J. M., Nimbus-7 CZCS: Electronic overshoot due to cloud reflectance. *Appl. Opt.*, *27*, 438–440, 1988.

Patterson, E. M., Optical properties of crustal aerosol: Relation to chemical and physical characteristics, *J. Geophys. Res.*, *86*, 3236–3246, 1981.

Patterson, E. M., C. S. Kiang, A. C. Delaney, A. F. Wartburg, A. C. D. Leslie, and B. J. Huebert, Global measurements in remote continental and marine regions: Concentrations, size distributions, and optical properties, *J. Geophys. Res.*, *85*, 7361–7376, 1980.

Prospero, J. M., and T. N. Carlson, Vertical and areal distribution of Saharan dust over the western equatorial North Atlantic Ocean. *J. Geophys. Res.*, *77*, 5255–5265, 1972.

Savoie, D. L., and J. M. Prospero, Aerosol concentration statistics for the northern tropical Atlantic, *J. Geophys. Res.*, *82*, 5954–5964, 1977.

Strang, G., *Introduction to Applied Mathematics*, 758 pp., Wellesley-Cambridge Press, Wellesley, Mass., 1986.

Tanre, D., M. Herman, P. Y. Deschamps, and A. deLeffe, Atmospheric modeling for space measurements of ground reflectances, including bidirectional properties, *Appl. Opt.*, *18*, 3587–3594, 1979.

Van de Hulst, H. C., *Light Scattering by Small Particles*, 470 pp., Dover, New York, 1957.

K. L. Carder and D. K. Costello, Department of Marine Science, University of South Florida, 140 Seventh Avenue, South, Saint Petersburg, FL 33701.

W. W. Gregg, Research and Data Systems, Greenbelt, MD 20770.

K. Haddad, Marine Research Laboratory, Florida Department of Natural Resources, Saint Petersburg, FL 33701.

J. M. Prospero, Rosenstiel School of Marine and Atmospheric Science, University of Miami, Miami, FL 33149.

(Received March 1, 1988;
revised March 1, 1989;
accepted October 19, 1989.)